Thermal and Scanning Electron Microscopy/Energy-Dispersive Spectroscopy Analysis of Styrene–Butadiene Rubber–Butadiene Rubber/Silicon Dioxide and Styrene–Butadiene Rubber–Butadiene Rubber/Carbon Black–Silicon Dioxide Composites

S. A. S. Venter,[1] M. H. Kunita,[1] R. Matos,[1] R. C. Nery,[2] E. Radovanovic,[1] E. C. Muniz,[1] E. M. Girotto,[1] A. F. Rubira[1]

[1]*Departamento de Química, Universidade Estadual de Maringá, Avenida Colombo 5790, 87020-900, Maringá, Pr, Brazil*
[2]*Departamento de Física, Universidade Estadual de Maringá, Avenida Colombo 5790, 87020-900, Maringá, Pr, Brazil*

Received 9 March 2004; accepted 28 May 2004
DOI 10.1002/app.21111
Published online in Wiley InterScience (www.interscience.wiley.com).

ABSTRACT: Silica as a reinforcement filler for automotive tires is used to reduce the friction between precured treads and roads. This results in lower fuel consumption and reduced emissions of pollutant gases. In this work, the existing physical interactions between the filler and elastomer were analyzed through the extraction of the sol phase of styrene–butadiene rubber (SBR)–butadiene rubber (BR)/SiO_2 composites. The extraction of the sol phase from samples filled with carbon black was also studied. The activation energy (E_a) was calculated from differential thermogravimetry curves obtained during pyrolysis analysis. For the SBR–BR blend, E_a was 315 kJ/mol. The values obtained for the composites containing 20 and 30 parts of silica per hundred parts of rubber were 231 and 197 kJ/mol, respectively. These results indicated an increasing filler–filler interaction, instead of filler–polymer interactions, with respect to the more charged composite. A microscopic analysis with energy-dispersive spectroscopy showed silica agglomerates and matched the decreasing E_a values for the SBR–BR/30SiO_2 composite well. © 2005 Wiley Periodicals, Inc. J Appl Polym Sci 96: 2273–2279, 2005

Key words: composites; elastomers; rubber; silicas; thermal properties

INTRODUCTION

In the formulations of treads for automotive tires, an exact understanding of the filler–polymer interactions enables optimum formulations, which lead to maximum synergic effects. The physical crosslinking provided by fillers in final composites combines with chemical vulcanization crosslinking and imparts better mechanical properties to the final product.[1–3]

Throughout the world, environmental concerns have given rise to green tires, that is, formulas for treads with a combination of silica and carbon black. According to recent studies, such tires reduce fuel consumption by approximately 6% and provide reduced emissions of pollutants.[4–7]

Correspondence to: A. F. Rubira (afrubira@uem.br).
Contract grant sponsor: Coordenação de Aperfeiçoamento de Pessoal de Nível Superior.
Contract grant sponsor: Conselho Nacional de Desenvolvimento Cientifico e Tecnológico (PROFIX project); contract grant number: 541058/01-0.

The main disadvantage of using silica is its higher cost with respect to carbon black. Moreover, the high surface polarity of silica, due to silanol groups, leads to the formation of hydrogen bonds, and this leads to the formation of silica agglomerates.[8] To make compatible the filler polarity and the apolarity displayed by most elastomeric matrices used in these systems, we could use bis(3-triethoxysilylpropyl) tetrasulfide (Si69, Degussa, São Paulo, Brazil) to modify the surface polarity of the silica.[9–11] However, the use of Si69 in the formulation of tires containing silica leads to a more expensive final product. Tires containing only carbon black do not require this extra additive.

Differential thermogravimetry (DTG) curves are often used to characterize elastomers and filled blends or composites; small changes in the thermogravimetry (TG) profile are magnified by its first derivative. For styrene–butadiene rubber (SBR) and butadiene rubber (BR), Sircar and Lamond[12] showed that the maximum degradation rate occurs at 720 and 738 K, respectively.[13–15]

When rubber stuffs are filled, a partially soluble composite is obtained; this is the extract called *unbound rubber*, which is composed of polymeric chains and filler-adsorbed polymeric chains; the gel phase is

TABLE I
Mass Loss for the SBR–BR/Filler Composites after Successive Extractions

Composite	Filler content (phr)	BdR (±3.5%)
SBR–BR/N234	10	11.7
	20	23.5
	30	33.6
SBR–BR/SiO_2	10	13.9
	20	38.4
	30	27.5

named *bound rubber* (BdR).[16–19] Concerning the aforementioned studies, this contribution describes a study in which a blend of SBR and BR was filled with silica and carbon black with the aim of elucidating the interactions between the fillers and rubber. Moreover, we compared carbon black filled samples and unfilled rubber samples. Thus, liquid-phase extractions were performed to obtain the BdR content, and we investigated the kinetic parameters through thermal analysis and the homogeneity of the dispersion of silica particles into the rubber matrix with energy-dispersive spectroscopy (EDS). The results are discussed in terms of hydrogen bonding between silanol groups present on the silica surface, which is possibly associated with drawbacks in the kinetic parameters studied.

EXPERIMENTAL

Sample preparation

In a rubber mill, 65 phr SBR was mixed with 35 phr BR (where phr is parts per hundred parts of rubber), and the mixture was continued to be mixed for 15 min without heating. Soon after, the filler was added at a preweighed concentration of 10, 20, or 30 phr, and the blend was mixed for 15 min. The same procedure was used to obtain carbon black (N234) filled samples (65 phr) and carbon black/silica filled samples (50–15, 40–25, or 40–12 phr). To the 40–12 sample was also added 3 phr Si69. To compare the results, we also prepared pure rubber samples and an unfilled SBR–BR sample.

BdR and gel content determination

Rubber samples (1.0 g) were weighed in 180-mesh polyester pouches and transferred to a Soxhlet extractor with 200 mL of dry toluene. After a reflux of 4 h, the packed samples were dried in an air-flux chamber at 303 K for 4 h and left for 24 h in a silica-drying compartment. These extractions were carried out until a constant mass was achieved. To ensure that the mass loss was assigned only to the rubber sample, we also performed assays with empty polyester bags.

Thermogravimetric analysis (TGA)

TGA of the samples was performed on a Shimadzu TGA-50 (Kyoto, Japan). About 20 mg of each sample was heated in an alumina pan from room temperature to 973 K at 10 K/min in flowing nitrogen (50 mL/min). The first derivatives of the TG curves were analyzed in terms of the normalized mass loss ratio (α), maximum temperature of decomposition (T_{max}), reaction order (n), and activation energy (E_a). To circumvent a mass loss early on at 313 K for the samples containing silica, we performed a preheating treatment at 423 K for 30 min.

Microscopic analysis

Scanning electron microscopy was carried out with a JEOL JSM-T300 microscope (Tokyo, Japan) at an acceleration voltage of 20 kV. EDS on a Kα Si line at 1.74 eV was also performed.

Kinetic model

By applying Avrami's kinetic model to partial DTG curves, following a degradation solid pyrolysis equation derived elsewhere,[20] we could calculate the kinetic parameters for each event:

$$\frac{d\alpha}{dt} = K(T)f[\alpha(t)] \quad (1)$$

where K is the rate constant, T is the temperature, and t is the time. Among the many forms used to represent solid pyrolysis, the most used is $f[\alpha(t)] = (1 - \alpha)^n$, with n considered invariable during the process. If the degradation can be activated at a temperature lower than 1073 K, which is within the temperature range of the kinetic reaction, K can be obtained by the Arrhenius law:

$$K = A^{(-E_a/RT)} \quad (2)$$

where A is the pre-exponential factor, E_a is the activation energy, R is the universal gas constant, and T is the temperature.

By substituting K [eq. (2)] into eq. (1), considering $f[\alpha(t)] = (1 - \alpha)^n$, applying the chain rule formula, and substituting dT/dt with β, which represents the heat-

TABLE II
Mass Loss for the SBR–BR/234 and SBR–BR/N234–Silica Composites after Successive Extractions

Composite	N234–SiO_2 (phr)	BdR (±3.5%)
SBR–BR/N234–SiO_2	65–0	57.6
	50–15	59.1
	40–25	57.9

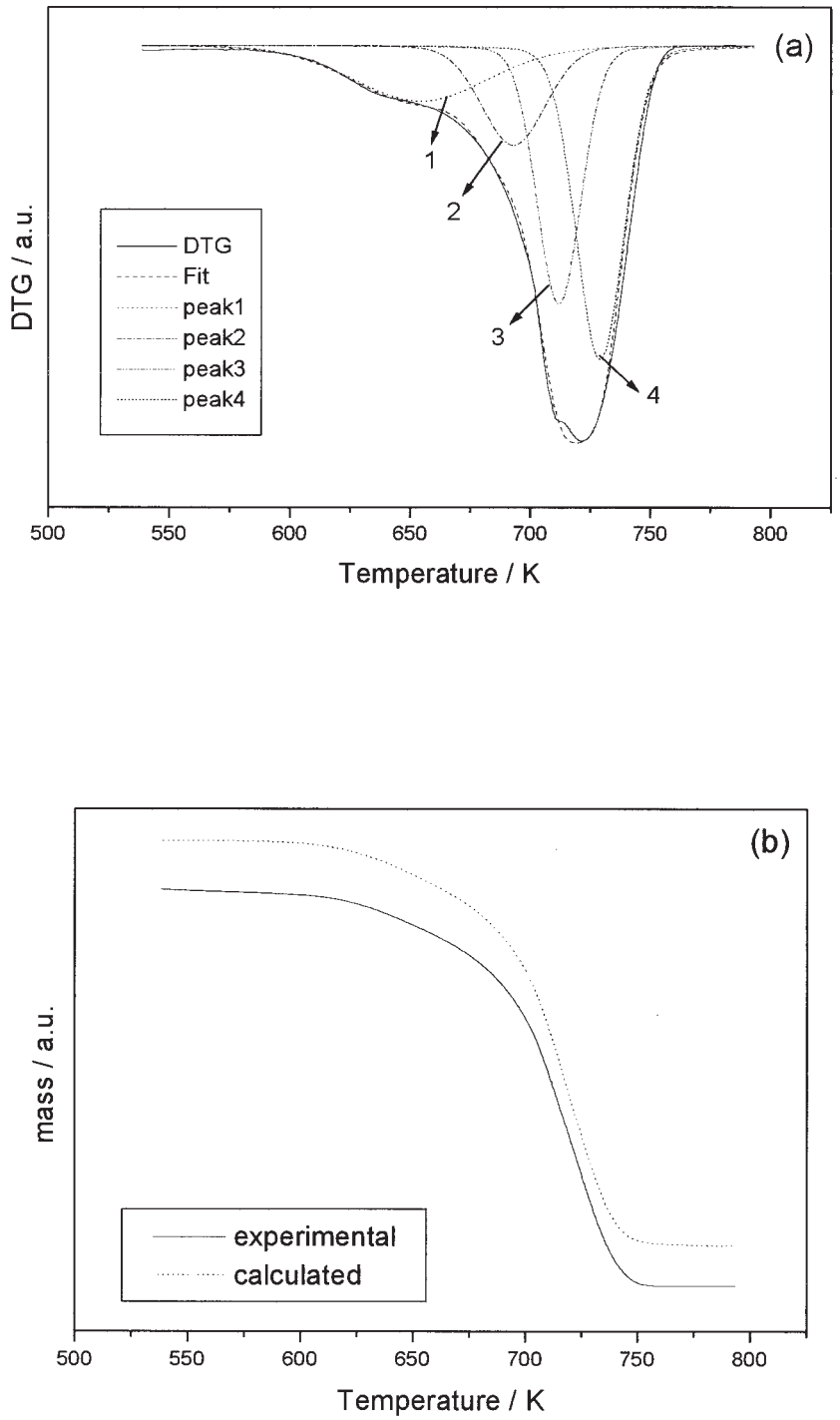

Figure 1 (a) Deconvolution procedure used for the DTG curve of an SBR–BR sample (heating rate = 10°C/min and N_2 flow rate = 50 cm^3/min and (b) experimental and calculated TG curves for an SBR–BR blend (one of the curves has been displaced for visualization).

ing rate, we transformed the linearized equation [eq. (1)] into

$$\ln\frac{d\alpha}{dT} - n\ln(1-\alpha) = \ln\frac{A}{\beta} - \frac{E_a}{R}\frac{1}{T} \qquad (3)$$

Using eq. (3), we calculated theoretically the kinetic parameters E_a, n, α, and T_{max}.

RESULTS AND DISCUSSION

Table I shows the BdR data for the SBR–BR/silica and SBR–BR/N234 composites after successive extractions in toluene. Samples containing 10 phr filler showed a greater mass loss, which indicated that these samples did not completely reach polymer–filler gel formation. For the SBR–BR/N234 samples, all the experiments

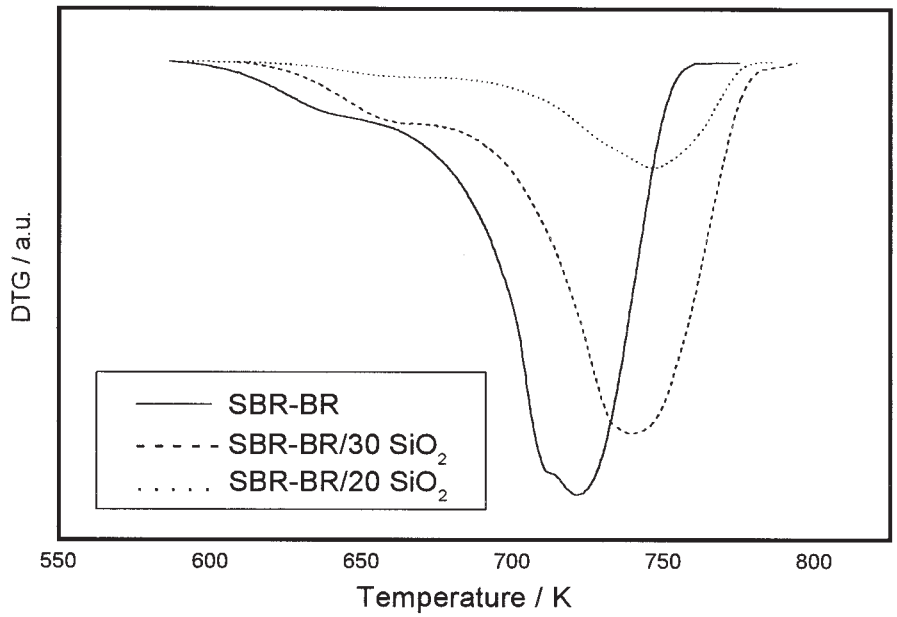

Figure 2 DTG curves for SBR–BR and its composites with silica.

showed an increasing BdR content with an increasing filler concentration. Thus, we could not determine the filler quantity at which all the filler particles became part of a coherent polymer–filler gel and could not be eluted by the solvent. For the silica composites, BdR decreasing with an increasing filler content from 20 to 30 phr suggested less effective filler–polymer interactions.[18,19,21,22] This could be assigned to the high surface polarity of the silica particles, due to silanol groups, which led to the formation of an agglomerated structure provided by hydrogen bonds between the Si—OH groups. In fact, this behavior was not observed in the samples containing carbon black. According to Choi,[21] when silica and curatives are incorporated into diene rubbers through mechanical mixing, a small amount of chemically BdR is usually formed that is negligible. In this work, the rubber gel was also negligible because the samples were not prepared with curatives or coupling agents, which would have chemically provided BdR.

Table II displays the BdR values for composites formed by carbon black/silica filled SBR–BR blends. We expected a decreasing BdR concentration in the more filled silica sample with respect to the data in Table I. However, a significant difference in the BdR concentration among the analyzed samples was not observed. This was probably due to a synergic effect occurring in the samples containing both silica and N234 fillers. After the measurements, full-combustion tests showed that all the silica used in the initial formulation was within the polymer–filler gel.

The degradation process of the SBR–BR blend has not been fully reported. Its pyrolysis presents several simultaneous events.[14,15] In an attempt to elucidate the SBR–BR degradation process, we used the deconvolution of DTG curves because every partial DTG describes a unique degradation event.

The theoretical TG was obtained from the sum of the partial TG curves. Through a point numerical integration it is possible to construct the partial TG curves from the DTG partial ones:[23]

$$AR = \lim_{\Delta x \to 0} \sum_{i=1}^{n} \frac{(x_{i+1} - x_i)(y_i + y_{i+1})}{2} \qquad (4)$$

where x and y correspond to the abscissa and ordinate when using the numerical integration through a trapezoidal method and AR is the trapezium area.

TABLE III
E_a and $T_{10\%}$ for the Blend and Composites

Sample	$T_{10\%}$ (K)	E_a (kJ/mol)
SBR–BR	642	315
SBR–BR/20SiO_2	672	231
SBR–BR/30SiO_2	665	197

TABLE IV
E_a for the Blends, Composites, and Gel Phase

N234–SiO_2, (phr)	E_a (kJ/mol)	
	Composite	Gel phase
65–0	181	181
50–15	151	154
40–25	159	137

With eq. (4), we could obtain the point integration of the partial DTG curves and the partial TG curves.

Figure 1(a) shows a deconvoluted DTG curve for which four events for the pyrolysis process of the SBR–BR blend have been assumed, and Figure 1(b) was obtained through the application of the aforementioned concepts [eq. (4)]. With Figure 1(a), the total E_a value of 315 kJ/mol was evaluated from the sum of the E_a values from partial DTG curves multiplied by the respective area percentages (pondered mean values). The experimental data and the predicted values calculated with the kinetic model adopted in this work agreed very well [Fig. 1(b)]. For this reason, all the kinetic parameters for the filled samples and their gels were extracted with the same mathematical procedure.

The normalized DTG curves for the SBR–BR blend filled with SiO_2 and without a filler are shown in Figure 2. By comparing the curves, we concluded that the higher thermal stability of the SBR–Br/SiO_2 samples was due to the physical crosslinking provided by the filler.[6,7] In addition, a higher temperature of degradation was found for a blend containing 20 phr SiO_2, and this was supported by data in Table I.

Table III presents the E_a values and the temperature of 10% degradation ($T_{10\%}$) for the SBR–BR and SBR–BR/SiO_2 samples. The sample containing 20 phr SiO_2 had higher E_a and $T_{10\%}$ values. Moreover, the SBR–BR/30SiO_2 blend (30 phr SiO_2) presented the lowest values with respect to the blends. These data suggest the existence of competing filler–filler and filler–polymer interactions, the latter being responsible for the physical crosslinking in the composite.[6,7,10] Table IV shows E_a data for samples containing both SiO_2 and carbon black as fillers and a sample containing only carbon black. Comparing the E_a values of the composite and the gel phase, we found that only the 40–25 polymer–filler gel showed a noticeable drop in E_a. This could be attributed to increasing filler–filler interactions when about 40% (Table II) of the unbound material was extracted; this led to an inhomogeneous SiO_2 distribution because of closer contact between the silica particles.[4,5,8]

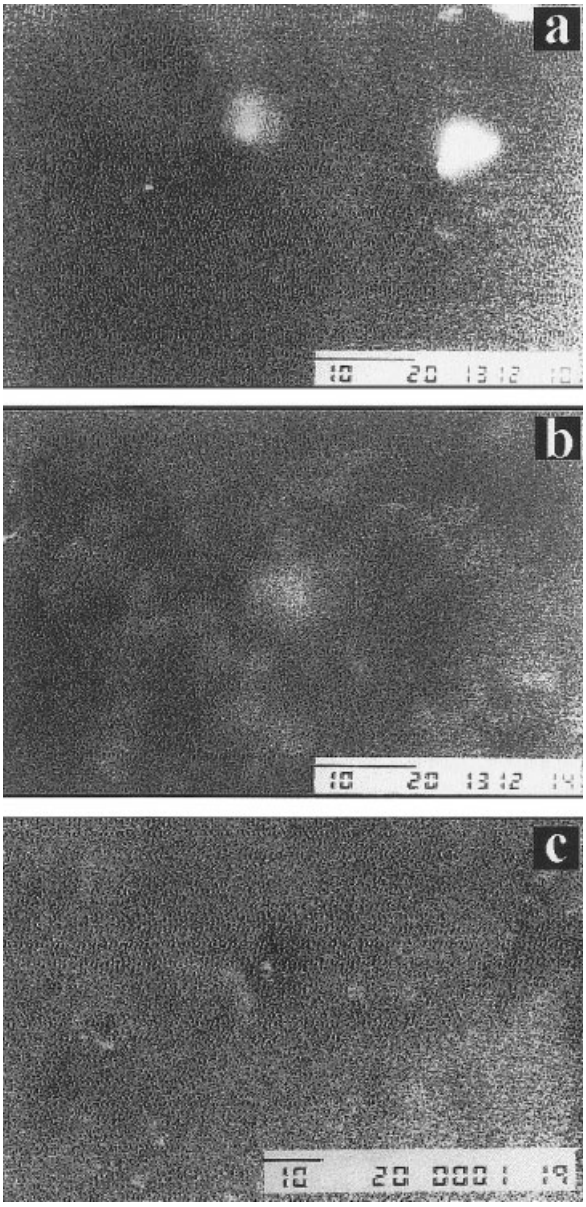

Figure 3 Si Kα EDS micrographs of blends containing (a) 20 phr SiO_2, (b) 30 phr SiO_2 (original magnification = 2000×), and (c) 30 phr SiO_2 and 3 phr Si69 (original magnification = 1000×). The bright spots are due to nondispersed charges.

EDS was used to analyze the SiO_2 dispersion (through Si Kα signals) in the composites and their gels (Fig. 3). The small, white points show the formation of SiO_2 agglomerates [Fig. 3(b)], which cannot be seen in Figure 3(a). This detail agrees with the data from Table I, suggesting a higher BdR concentration for the SBR–BR/20SiO_2 sample. The effect of Si69 is verified in Figure 3(c), which presents a homogeneous dispersion of silica particles. In general, the EDS results in Figure 3 agree with Table III because the composite containing 20 phr silica showed better polymer–filler interactions. The possibility of agglomeration suggested by E_a decreasing for the 40–25 gel phase composite (Table IV) was investigated with EDS (Fig. 4). When the unbound material was extracted from the 50–15 sample [Fig. 4(a)], an increasing filler concentration was observed without a reduction in the silica homogeneity [Fig. 4(b)]. Otherwise, we observed silica agglomeration for the 40–25 gel phase [Fig. 4(d)], probably because of hydrogen bonding between silanol groups on the surface of the silica. Analogously, the EDS results in Figure 4 agree with the data in Table IV. Table IV also shows the E_a values

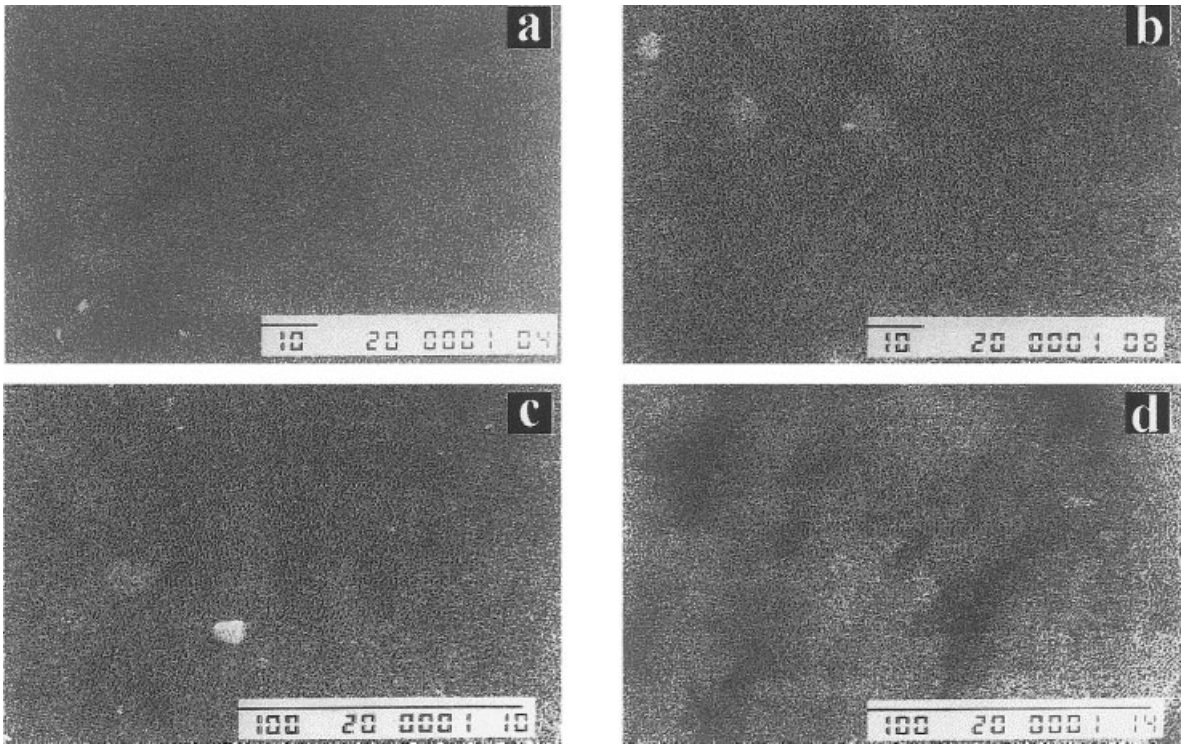

Figure 4 Si Kα EDS micrographs of composites with different N234–SiO_2 concentrations (phr): (a) 50–15, (b) gel phase of 50–15 (original magnification = 1000×), (c) 40–25, and (d) gel phase of 40–25 (original magnification = 500×). The bright spots are due to nondispersed charges.

with respect to the N234 and SiO_2 concentrations. For the composite, the decrease in the N234 content reduced E_a because of the smaller amount of the gel phase. For the gel phase, the increase in the SiO_2 concentration reduced E_a because of the agglomeration of silica particles. Thus, a compensation-like effect in the composite could be suggested, but this was not applicable to the gel phase because of the silica agglomeration effect, which was observed with EDS. In addition, the results suggested that the E_a drop for the gel phase was mostly attributable to SiO_2 agglomeration; otherwise, the changes (50–15 to 40–25) in E_a for the composite would be similar.

CONCLUSIONS

The results of this study indicated better polymer–filler interactions for SBR–BR/20SiO_2 samples because of improved silica dispersion within the elastomer. A decreasing BdR concentration indicated filler–filler interactions because of the approximation of the filler particles, and this led to the formation of agglomerates. This fact was also verified with thermal analysis data.

Silica and carbon black as reinforcement fillers should not be used in excess of 20 phr SiO_2 to prevent the formation of competing SiO_2–SiO_2 and SiO_2–polymer interactions.[9,10,24]

Although the formation mechanisms of the polymer–filler gel were different from those of the rubber and carbon black and the rubber and silica, the BdR and TGA results, along with the EDS analysis, could be used to estimate the degree of physical interactions. In addition, we could not neglect the changes in the carbon black concentration if we wanted to understand and explain the E_a changes.

Despite the differences in the polymer–silica interactions of the two repeat units and the differences in the bond dissociation energies, data in the literature suggest stronger interactions between BR and silica.[21] In this work, we used blends of 65 phr SBR (SBR 1502, with 23.5% styrene) and 35 phr BR; thus, the blends contained about 15 wt % styrene. Hence, the differences in the polymer–filler interactions were minimized and did not affect the conclusions. Finally, the mathematical procedure used for the experimental data allowed us to determine kinetic parameters that were in good agreement with the reported data.

The authors thank Rank Pneus, Ltd., for its donation of rubber samples and the Instituto de Química (Unicamp) for the energy-dispersive spectroscopy analysis.

References

1. Strong, A. B. Plastics—Materials and Processing; Prentice Hall: Upper Saddle River, NJ, 1996.
2. Ohm, R. F. The Vanderbilt Rubber Handbook, 13th ed.; Vanderbilt: Norwalk, CT, 1990.
3. Kirk, R. E.; Othmer, F. Encyclopedia of Chemical Technology, 3rd ed.; Wiley: New York, 1982; Vol. 20.
4. Waddel, W. H.; Evans, L. R. Rubber Chem Technol 1996, 69, 377.
5. Wang, M. J.; Mahmud, K.; Murphy, L. J.; Patterson, W. J. Kautsch Gummi Kunstst 1998, 51, 348.
6. Yatsuyanagi, F.; Suzuki, N.; Ito, M.; Kaidou, H. Polymer 2001, 42, 9523.
7. Donnet, J. B. Rubber Chem Technol 1998, 71, 323.
8. Waddell, W. H.; Evans, L. R.; Goralski, E. G.; Snodgrass, L. J. Rubber Chem Technol 1996, 69, 48.
9. Sheng, E.; Sutherland, I.; Bradley, R. H.; Freakley, P. K. Eur Polym J 1996, 32, 35.
10. Choi, S. S.; Kim, I. S. Eur Polym J 2002, 38, 1265.
11. Choi, S. S. Polym Test 2002, 21, 201.
12. Sircar, A. K.; Lamond, T. G. Rubber Chem Technol 1978, 51, 647.
13. Hatakeyama, T.; Quinn, F. Thermal Analysis—Fundamentals and Applications to Polymer Science; Wiley: Chichester, England, 1994.
14. Choi, S. S. J Anal Appl Pyrolysis 2001, 57, 249.
15. Lin, J.; Chang, C.; Wu, C.; Shih, S. Polym Degrad Stab 1996, 53, 295.
16. Meissner, B. J Appl Polym Sci 1974, 18, 2483.
17. Meissner, B. J Appl Polym Sci 1993, 50, 285.
18. Meissner, B.; Karasék, L. J Appl Polym Sci 1994, 52, 1925.
19. Meissner, B.; Karasék, L. J Appl Polym Sci 1998, 69, 95.
20. Wendlandt, W. W. Thermal Analysis; Wiley: New York, 1986.
21. Choi, S. S. J Anal Appl Pyrolysis 2000, 55, 161.
22. Leblanc, J. L. Prog Polym Sci 2002, 27, 627.
23. Taylor, H. E.; Wade, T. L. Cálculo Diferencial e Integral, 3rd ed.; Wiley: Mexico, 1965.
24. Stevenson, I.; David, L.; Gauthier, C.; Arambourg, L.; Davenas, J.; Vigier, G. Polymer 2001, 42, 9287.